AgriEngineering

MDPI

Article

Vegetation Indices Applied to Suborbital Multispectral Images of Healthy Coffee and Coffee Infested with Coffee Leaf Miner

Luana Mendes dos Santos [1], Gabriel Araújo e Silva Ferraz [1,*], Diego Bedin Marin [1], Milene Alves de Figueiredo Carvalho [2], Jessica Ellen Lima Dias [3], Ademilson de Oliveira Alecrim [4] and Mirian de Lourdes Oliveira e Silva [1]

[1] Agricultural Engineering Department, Federal University of Lavras, Lavras 37200-000, MG, Brazil; luanna_mendess@yahoo.com.br (L.M.d.S.); db.marin@hotmail.com (D.B.M.); olivemiri@gmail.com (M.d.L.O.e.S.)
[2] Embrapa Café, Brasília 70770-901, DF, Brazil; milene.carvalho@embrapa.br
[3] Department of Agriculture and Environmental Sciences, Hungarian University of Agriculture and Life Sciences, 2100 Budapest, Hungary; lima.dias.jessica.ellen@stud.uni-mate.hu
[4] Department of Agronomy, Faculty of Sciences and Technologies of Campos Gerais (FACICA), Campos Gerais 37160-000, MG, Brazil; ademilsonagronomia@gmail.com
* Correspondence: gabriel.ferraz@ufla.br

Abstract: The coffee leaf miner (*Leucoptera coffeella*) is a primary pest for coffee plants. The attack of this pest reduces the photosynthetic area of the leaves due to necrosis, causing premature leaf falling, decreasing the yield and the lifespan of the plant. Therefore, this study aims to analyze vegetation indices (VI) from images of healthy coffee leaves and those infested by coffee leaf miner, obtained using a multispectral camera, mainly to differentiate and detect infested areas. The study was conducted in two distinct locations: At a farm, where the camera was coupled to a remotely piloted aircraft (RPA) flying at a 3 m altitude from the soil surface; and the second location, in a greenhouse, where the images were obtained manually at a 0.5 m altitude from the support of the plant vessels, in which only healthy plants were located. For the image processing, arithmetic operations with the spectral bands were calculated using the "Raster Calculator" obtaining the indices NormNIR, Normalized Difference Vegetation Index (NDVI), Green-Red NDVI (GRNDVI), and Green NDVI (GNDVI), the values of which on average for healthy leaves were: 0.66; 0.64; 0.32, and 0.55 and for infested leaves: 0.53; 0.41; 0.06, and 0.37 respectively. The analysis concluded that healthy leaves presented higher values of VIs when compared to infested leaves. The index GRNDVI was the one that better differentiated infested leaves from the healthy ones.

Keywords: precision agriculture; *Coffea arabica* L.; remote sensing; unmanned aerial vehicles (UAV); digital agriculture

Citation: Santos, L.M.d.; Ferraz, G.A.e.S.; Marin, D.B.; Carvalho, M.A.d.F.; Dias, J.E.L.; Alecrim, A.d.O.; Silva, M.d.L.O.e. Vegetation Indices Applied to Suborbital Multispectral Images of Healthy Coffee and Coffee Infested with Coffee Leaf Miner. *AgriEngineering* **2022**, *4*, 311–319. https://doi.org/10.3390/agriengineering4010021

Academic Editor: Mohammad Valipour

Received: 26 January 2022
Accepted: 15 March 2022
Published: 17 March 2022

1. Introduction

Brazil is currently the largest coffee exporter in the world. The estimation for the 2020/2021 harvest globally is 175.5 million sacks (60 kg each) [1]. Within that amount, the state of Minas Gerais is highly significant. In 2019, the state of Gerais produced the highest amount with 34.6 million sacks of post-processed grain, summing 55% of the whole Brazilian production [2].

Globally, coffee has had an increase in consumption advancing the market even during the COVID-19 pandemic; 7 of 13 studies indicated an increase, accounting for 53.8% [3]. German outpatient care givers also reported higher coffee consumption [4]. In Poland, the highest frequency of coffee consumption (88.9%) was among adults aged 45+ but referring only to COVID-19 confinement [5].

It is estimated that this year's demand is rising by 1.5% worldwide, in comparison to the previous year; this percentage represents 2.5 million sacks [1]. Therefore, with the

increase of consumption, coffee farmers are likely to face challenges to supply the demand, by increasing the efficiency and the production of the seed.

With the increase of production areas, the coffee plants become a major host of a variety of arthropods, which are considered pests with great economic impact, causing direct and indirect damages [3]. The coffee leaf miner (*Leucoptera coffeella*) is considered a primary pest that attacks coffee plants during the whole year, especially in hot and dry seasons [4].

The coffee leaf miner, a small silvery-white moth with a diurnal mating habit, hides in the foliage during the day and lays an average of seven eggs per day on the surface of the leaves [6]. The development of the eggs varies from 5 to 21 days according to the temperature, when they hatch they penetrate the epidermis of the leaf to feed and to form "mines". Mines are light brown in color with a rounded shape, reaching a darker color due to the accumulation of excretions [6]. The attack of the coffee leaf miner reduces the photosynthetic area of the leaves, thus reducing seed production and decreasing the yield [7].

With advances in precision agriculture and the emergence of remote sensing aerial platforms, such as unmanned aerial systems (UAS), also known as remotely piloted aircraft (RPA) or unmanned aerial vehicles (UAV), details of the study area can be obtained. In addition, such platforms provide accurate information of the culture and in a timely manner for corrective actions [8].

It is worth mentioning the advantages of using several optical sensors embedded in this type of aerial platform. From being possible to using the different bands of these sensors to calculate vegetation indices (VI), such as the study by Bento [8], in which the authors applied different VI for characterizing three recently planted coffee cultivars (*Coffea arabica* L.) in addition to verifying the influence of rain and drought on the development of biophysical variables measured in the field. Barbosa [9] evaluated the potential of the practical application of unmanned aerial vehicles and RGB vegetation indices (VIs) in the monitoring of a coffee crop. To identify field anomalies and obtaining more information on disease, Marin [10] proposed a framework to detect coffee rust severity with only vegetation indices extracted from RPA images.

In this context, the processing of images obtained from multispectral cameras, resulting in VI, can be obtained using mathematical equation of two or more wavelength reflectance, commonly in the visible spectral region, in red edge, and near-infrared region [11].

Furthermore, VI are commonly used in agricultural monitoring due to their power to highlight the intrinsic characteristics of the vegetation, which are related to the reflection of green by the plants, reflecting their vigor status [12].

Therefore, vegetation indices are a strategic tool to aid the early detection of pests and diseases, contributing to effective phytosanitary control and management of coffee plantations.

Some studies on the use of VI from RPA camera images are under development, such as disease is coffee leaf rust (CLR) detection [10,13] and nematode detection [14]. In the case of a pest like the coffee leaf miners, research is still incipient and less widespread in the literature, however it has fundamental economic importance, highlighting the importance of the applicability and development of the proposed study.

As a hypothesis of this research, it possible to identify the infestation of coffee leaf miners in newly planted coffee plants using VI and images obtained by RPA. This study aimed to assess the VI values from images obtained with a multispectral camera in healthy leaves and infested leaves by coffee leaf miners of recently established coffee plants to detect and differentiate the infestation of the pest.

2. Materials and Methods

The study was carried out in two separate locations. Five healthy coffee plants (*Coffea arabica*) were grown in a greenhouse setup. For the infested plants, 5 plants used were located in the coffee plantation. Healthy leaves of coffee (*Coffea arabica* L.) of the Catuai-IAC66 cultivar were sampled from 1-month-old plants in the greenhouse at the campus of the Federal University of Lavras (UFLA; 21°13′33″ S, 44°58′17″ W), south of Minas Gerais.

Coffee leaf miner infested leaves were sampled from 8-month-old plants at the Cafua farm, in the municipality of Ijaci, south of Minas Gerais, in an area of 0.3 ha of coffee plantation (*Coffea arabica* L.) of the Catuaí Vermelho IAC 99 cultivar, planted in November 2018, with spacing 3.5 m between rows and 0.5 m between plants. The geographic coordinates are 21°9′50″ S and 44°59′35″ W, with an average altitude of 934 m in the city of Ijaci, southern region of Minas Gerais (Figure 1).

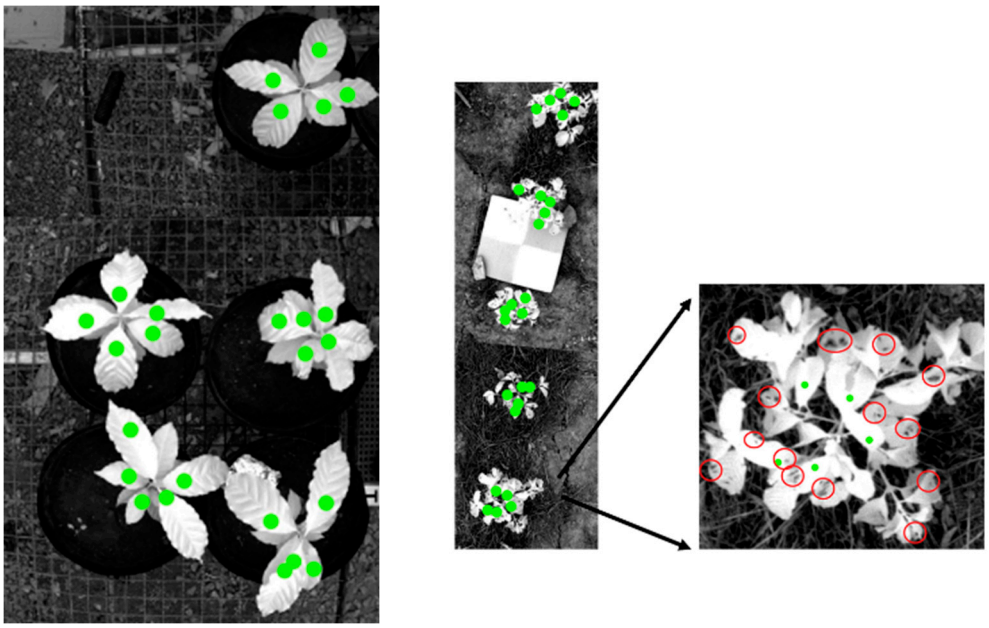

(**A**) (**B**)

Figure 1. Images of the near-infrared band (NIR), obtained with a multispectral camera. (**A**): Leaves of healthy plants in the greenhouse and the green dots represent sampled points. (**B**): Leaves of infested plants in the field and the green dots represent sampled points. Zoomed area of one of the plants, where the red circles represent the coffee leaf miners.

The climate of the region, according to the Koppen classification, is of the Monsoon-influenced humid subtropical climate (Cwa) type, characterized by a dry season in winter and a rainy season in summer, with an average temperature of 20 °C and average annual rainfall of 1153 mm [15].

In the field, the camera Parrot SequoiaTM (Parrot S.A., Paris, France) was coupled to a RPA, model 3DRSolo (3DR Robotics, Berkeley, CA, USA) (Figure 2a), equipped with a rotating wing platform. The flight was performed at a height of 3 m from the infested plants. This height was adopted after height tests carried out in the field. The images were analyzed and because it was possible to visualize the mines without changing the resolution in the images, this flight height was used. In the greenhouse, the photos were taken manually at a height of 0.5 m from the support where the vessels of healthy plants were located. This height was adopted due to the low height of the greenhouse.

The images were captured by the multispectral camera, which has four spectral sensors with a resolution of 1.2 MP, as shown in Table 1 and Figure 2b. The sensors are auto calibrated through a solar sensor (Sunshine Sensor) integrated into the camera, with an image size of 1280 × 960 pixels, and an RGB sensor with a resolution of 16 MP, which in this study were not used. The sunlight sensor corrects images in different lighting conditions by measuring solar irradiance. The sensor includes a global positioning system (GPS) receiver and IMU (inertial measurement unit) to measure the position and orientation of the sensor when capturing images [16].

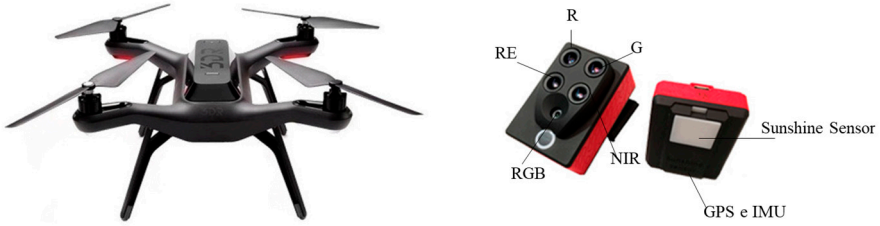

Figure 2. Equipment: (**a**) RPA used for the field survey; (**b**) camera, and sensors of imagery and irradiance.

Table 1. Characteristics of the spectral bands used in the study.

Band	Initial λ (nm)	Final λ (nm)
Green (G)	530	570
Red (R)	640	680
Red Edge (RE)	730	740
Near Infrared (NIR)	770	810

λ—wavelength.

The images were processed in the software QGIS version 3.10 [17]. Arithmetic operations were performed using the Raster Calculator for the R, NIR, and G bands based on the VIs described in Table 2.

Table 2. Vegetation indices calculated from multispectral bands of the acquired images.

Vegetation Indices (VI)	Equation	Reference
Normalized Difference Vegetation Index (NDVI)	$NDVI = \frac{NIR-R}{NIR-R}$	[18]
Green Normalized Difference Vegetation Index (GNDVI)	$GNDVI = \frac{NIR-G}{NIR-G}$	[19]
Norm NIR	$NormNIR = \frac{NIR}{NIR+R+G}$	[20]
Green-Red NDVI	$GRNDVI = \frac{NIR-(G+R)}{NIR+(G+R)}$	[21]

For the image processing, a total of 50 pixels points were randomly sampled, 25 points from healthy leaves and 25 points from infested plants. In addition, 41 points were sampled in the mines of infested plants. The mines have different sizes, ranging from 1 to 2 cm in diameter. Plants with 20% to 30% of leaves with intact mines (with live caterpillars) in the middle and upper thirds were considered as infested.

To obtain the results of the VIs in the pixels of the sampled points, the Point Sampling Tools plugin was used. Information was extracted from a single pixel, using the plugin. Due to the high spatial resolution, no mixed pixels were observed.

From the VI values, descriptive statistical analysis was performed on the results by the Shapiro–Wilk normality test (W; $p < 0.05$). The values of Vis that showed normal distribution were subjected to the *t*-test ($p < 0.05$), to identify significant differences in the different Vis used. The statistical analysis was conducted using R software (R Core Team, Vienna, Austria).

The layouts of Figures were made in QGIS version 3.10 [17] of the compositions of the VIs of the studied area for better visualization, understanding of the vegetation canopy, and assisting in the analysis of the vegetation indices.

3. Results and Discussion

Table 3 shows the statistical summary of the VI values obtained in the study. The result of the normality test is also presented in Table 3. Non-normal distribution was observed for

NDVI in healthy and infested leaves and GNDVI in healthy leaves. Thus, the mean values of those VIs were not compared with the others.

Table 3. Summary of descriptive statistic values for VIs in healthy leaves and infested leaves, in the greenhouse and the farm. VIs values in the mines of infested plants, in the farm.

VI	State of the Leaf	n	Average	SD	Min	Max	W	*p*-Value
NDVI	Infested	41	0.41	0.15	−0.04	0.64	0.90	0.00
	Healthy	50	0.64	0.15	−0.01	0.79	0.89	0.00
GNDVI	Infested	41	0.37	0.15	−0.01	0.63	0.97	0.27
	Healthy	50	0.55	0.16	0.17	0.77	0.97	0.05
NormNIR	Infested	41	0.53	0.07	0.36	0.65	0.96	0.20
	Healthy	50	0.66	0.08	0.38	0.79	0.98	0.17
GRNDVI	Infested	41	0.06	0.15	−0.28	0.3	0.96	0.20
	Healthy	50	0.32	0.17	−0.23	0.57	0.98	0.17

n—number of observations, SD—standard deviation, Min—minimum VI value, Max—maximum VI value and W—Shapiro Wilk normality test.

Figure 3 shows the Box-plot for the VI values calculated from the greenhouse and the farm. VI values were slightly higher on the healthy leaves in the greenhouse; though no significant difference ($p > 0.05$) between the locations was observed. This is because the infestation of coffee leaf miners in the farm was at the beginning and did not present intense damage. This result is related to the selectivity of the moths of this pest. The infested plants, or plants with mines of the coffee leaf miner bug, according to Nestel [22], are plants with greater vegetative vigor, preferred for oviposition of this pest. This explains the little variation in VI values in leaves of infested plants and healthy plants.

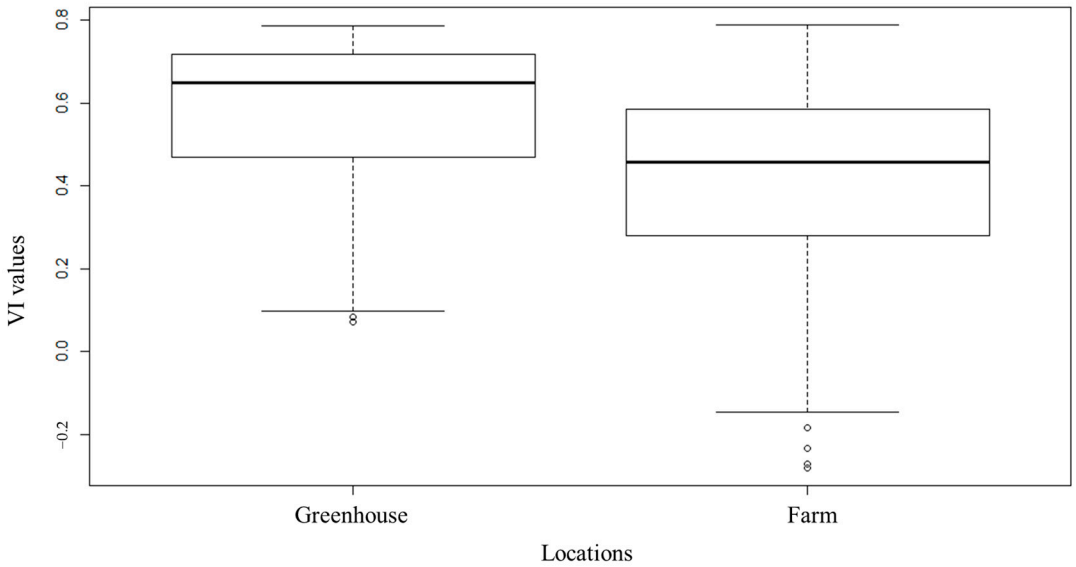

Figure 3. Box plots for VI values in the greenhouse and farm field, which do not show a statistically significant difference by *t*-test ($p > 0.05$).

According to Ahmed [23], the greater the vegetative vigor of the plants the lower the reflectance in the visible bands and higher in the near-infrared band. Additionally, plants with higher vegetative vigor have higher biomass content and higher nutrient content, showing higher VI values.

Figure 4 shows the Box-plot graphs for the values of VI as a function of location that showed a statistically significant difference by the *t*-test ($p < 0.05$). There are significant differences between the indices. The NormNIR index in healthy leaves showed the highest

value, and little variation between NormNIR values in healthy and infested plants was found. The result obtained by this VI also reflect the selectivity of the moths and the little variation of its values in leaves of infested plants and healthy plants.

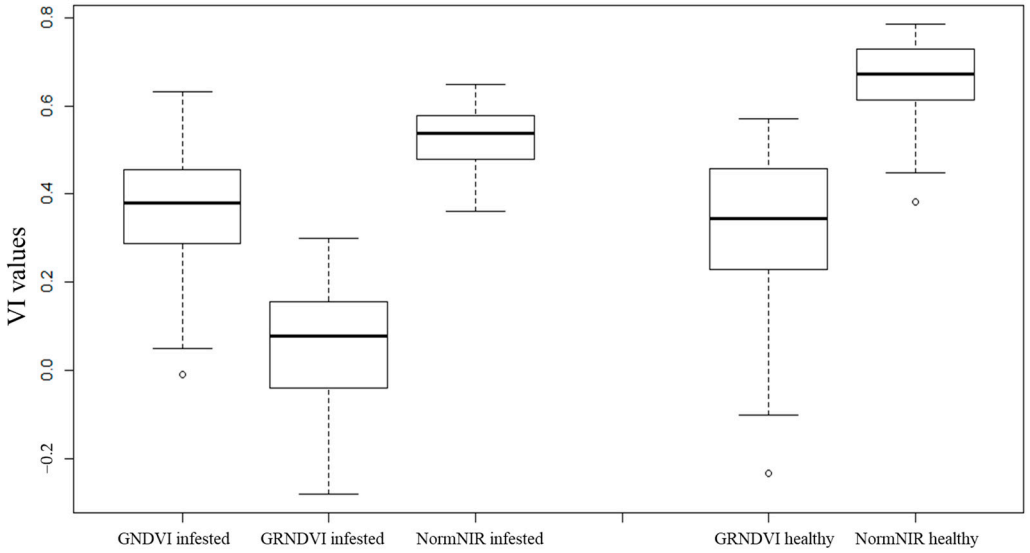

Figure 4. Box-plot for GRNDVI and NormNIR values in the greenhouse and farm field, that showed statistically significant difference by *t*-test ($p < 0.05$).

According to Marin [10], there is a direct and positive correlation of the coffee leaf miner infestation to the VI, this occurs in the initial stages of the attack of the pest, corroborating with this study. The result indicates that the infestation, even at the beginning, can be identified using VI.

The lowest values of VI were found in the GRNDVI for infested plants, and this VI also showed less variation in values for healthy and infested plants.

For situations where the infestation occurs at the beginning of the season, depending on the height of the flight and with low spatial resolution, the images collected may not show any advantage in the identification of the coffee leaf miner, as there may be mixed pixels and both infested and healthy plants may present close average values of VI. When the attack is intense, this pest reduces the photosynthetic capacity of the plant by the destruction and fall of leaves [6,24,25]. Consequently, the values of VIs tend to decrease, being possible to recognize the defoliation in the images. This fact was not observed in this study, because the attack of the coffee leaf miner was still in the beginning. Therefore, further work is recommended to follow the evolution of the pest and the response of the VIs.

It was visually verified that the VI values for healthy plants presented a more intense green coloration of the legend scale. Yet, infested plants in the field had some leaves with the same intense green coloration visualized in the maps below (Figure 5).

In Figure 5A,B, it is observed that there was not much variation in the VI values, remaining between 0.6 and 1. This result is due to the NormNIR VI feature that corrects spectral bands to normalize different illumination levels compared to absolute bands.

It is observed that in Figure 5C–E the GRNDVI and GNDVI resulted in lower values when compared to Figure 5A,B, this is due to the different operations performed with different bands. It is noteworthy that the scale of variation of the VI values was standardized to allow a comparison between them.

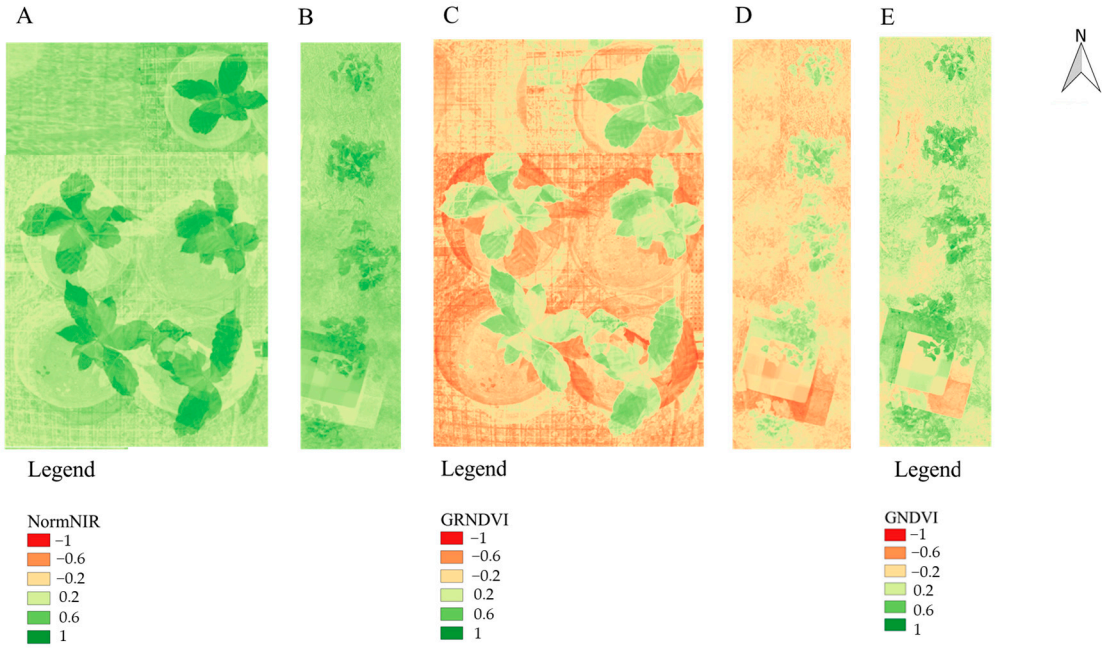

Figure 5. NormNIR Vegetation Index applied in the images (**A**): Healthy plants in the nursery, (**B**): infested plants in the field. GRNDVI applied in the images (**C**): healthy plants in the nursery, (**D**): plants infested in the field. GNDVI applied in the images (**E**): plants infested in the field.

The GNDVI in healthy leaves did not show the normal distribution and therefore was discarded from the comparisons. The NormNIR and GRNDVI observed significant differences in healthy and infested plants. By visual analysis, the GRNDVI was the VI that best differentiated healthy plants from infested plants (Figure 5C,D).

The VI values in the mines of the bugs were, on average, lower when compared to the VI values in healthy leaves. Additionally, some mines showed negative VI values, which are attributed to the darker coloration of the mines.

Figure 6 shows that the mines presented an accumulation of excretions that had a darker coloration, making the red reflectance value higher and consequently favoring the decrease in the VI values under study.

Figure 6. Infested plant in the field with mines of coffee leaf miner highlighted in red.

According to Franklin [6], the females of the coffee leaf miner oviposit on the upper side of the leaves, which hatch and penetrate the leaf epidermis, starting the feeding from the leaves and formation of the mines. The mines have a rounded shape and are colored light brown, the darker color is due to the accumulation of excretions.

We recommend future research on this topic to be carried out in areas with different levels of infestation. In addition, we recommend the use of deep learning algorithms and the random forest algorithm as in the studies by Marin [26] and Kagan [27].

4. Conclusions

It conclusion, that research showed that, on average, healthy plants showed higher VI values compared to infested plants. Additionally, GRNDVI best differentiated healthy plants from infested plants compared with other VIs.

Author Contributions: L.M.d.S.: conception of the research, data acquisition, data analysis and interpretation, preparation of the study, writing and review of the study; G.A.e.S.F.: supervision and review of the study; D.B.M.: data analysis, interpretation, and review of the study; M.A.d.F.C.: supervision and review of the study; J.E.L.D.: review of the study; A.d.O.A.: data acquisition; M.d.L.O.e.S. review of the study. All authors have read and agreed to the published version of the manuscript.

Funding: To Coffee Research Consortium EMBRAPA CAFÉ for funding the research and propagation of the study.

Institutional Review Board Statement: Not applicable.

Informed Consent Statement: Not applicable.

Data Availability Statement: Not applicable.

Acknowledgments: We would like to thank the Embrapa Brazilian Coffee Research Consortium, the National Council for Scientific and Technological Development (CNPq), the Coordination for the Improvement of Higher Education Personnel (CAPES), the Federal University of Lavras (UFLA), and the Farm Cafua.

Conflicts of Interest: The authors declare no conflict of interest.

References

1. United States Department of Agriculture (USDA). Available online: http://usda.mannlib.cornell.edu/MannUsda/viewDocumentInfo.do?documentID=1801 (accessed on 10 February 2021).
2. Conab-Companhia Nacional de Abastecimento. *Acompanhamento da Safra Brasileira de Café*; Conab-Companhia Nacional de Abastecimento: Brasília, Brazil, 2021; v.8, n.3.
3. Castellana, F.; De Nucci, S.; De Pergola, G.; Di Chito, M.; Lisco, G.; Triggiani, V.; Sardone, R.; Zupo, R. Trends in Coffee and Tea Consumption during the COVID-19 Pandemic. *Foods* **2021**, *10*, 2458. [CrossRef] [PubMed]
4. Mojtahedzadeh, N.; Neumann, F.A.; Rohwer, E.; Nienhaus, A.; Augustin, M.; Harth, V.; Zyriax, B.-C.; Mache, S. The Health Behaviour of German Outpatient Caregivers in Relation to the COVID-19 Pandemic: A Mixed-Methods Study. *Int. J. Environ. Res. Public Health* **2021**, *18*, 8213. [CrossRef] [PubMed]
5. Sidor, A.; Rzymski, P. Dietary Choices and Habits during COVID-19 Lockdown: Experience from Poland. *Nutrients* **2020**, *12*, 1657. [CrossRef] [PubMed]
6. Franklin, A.M.; Martins, F.K.; Costa, E.S.; Nunes, J.F. Comunidade de parasitóides associados ao Bicho-mineiro (*Leucoptera coffeella* Guérin-Mèneville) em folhas de café (*Coffea arábica* L.) cultivadas no Sudoeste de Minas Gerais. *Ciência ET Prax.* **2017**, *10*, 25–30.
7. Liska, G.R.; Silveira, E.C.D.; Reis, P.R.; Cirillo, M.Â.; Gonzalez, G.G.H. Seleção de um modelo de regressão binomial para taxa de predação de Euseius concordis (Chant, 1959). *Coffee Sci.* **2015**, *10*, 113–121.
8. Bento, N.L.; Ferraz, G.A.E.S.; Barata, R.A.P.; Soares, D.V.; Santos, L.M.D.; Santana, L.S.; Ferraz, P.F.P.; Conti, L.; Palchetti, E. Characterization of Recently Planted Coffee Cultivars from Vegetation Indices Obtained by a Remotely Piloted Aircraft System. *Sustainability* **2022**, *14*, 1446. [CrossRef]
9. Barbosa, B.D.S.; Araújo e Silva Ferraz, G.; Mendes dos Santos, L.; Santana, L.; Bedin Marin, D.; Rossi, G.; Conti, L. Aplicação de Imagens RGB Obtidas por VANT na Cafeicultura. *Remote Sens.* **2021**, *13*, 2397. [CrossRef]
10. Marin, D.B.; Santana, L.S.; Barbosa, B.D.S.; Barata, R.A.P.; Osco, L.P.; Ramos, A.P.M.; Guimarães, P.H.S. Detecting coffee leaf rust with UAV-based vegetation indices and decision tree machine learning models. *Comput. Electron. Agric.* **2021**, *190*, 106476. [CrossRef]

11. Wójtowicz, M.; Wójtowicz, A.; Piekarczyk, J. Application of remote sensing methods in agriculture. *Commun. Biometry Crop Sci.* **2016**, *11*, 31–50.
12. Martins, R.N.; Pinto, F.D.A.D.C.; de Queiroz, D.M.; Valente, D.S.M.; Rosas, J.T.F. Um novo índice de vegetação para monitoramento da maturação do café usando imagens aéreas. *Sens. Remote* **2021**, *13*, 263.
13. Velásquez, D.; Sánchez, A.; Sarmiento, S.; Toro, M.; Maiza, M.; Sierra, B. Um método para detectar a ferrugem do café através de redes de sensores sem fio, sensoriamento remoto e aprendizado profundo: Estudo de caso da variedade caturra na Colômbia. *Ciências Apl.* **2020**, *10*, 697.
14. Oliveira, A.J.; Assis, G.A.; Guizilini, V.; Faria, E.R.; Souza, J.R. Segmenting and Detecting Nematode in Coffee Crops Using Aerial Images. In *Transactions on Petri Nets and Other Models of Concurrency XV*; Springer Science and Business Media LLC.: Berlin/Heidelberg, Germany, 2019; pp. 274–283.
15. Alvares, C.A.; Stape, J.L.; Sentelhas, P.C.; Gonçalves, J.L.M.; Sparovek, G. Köppen's climate classification map for Brazil. *Meteorol. Z.* **2013**, *22*, 711–728. [CrossRef]
16. Olsson, P.O.; Vivekar, A.; Adler, K.; Garcia Millan, V.E.; Koc, A.; Alamrani, M.; Eklundh, L. Evaluating the accuracy of the parrot sequoia camera and sunshine sensor. *Remote Sens.* **2021**, *13*, 577. [CrossRef]
17. Qgis. Qgis Geographic Information System. Open Source Geospat. Found. Proj. 2016. Available online: http://qgis.osgeo.org (accessed on 10 June 2020).
18. Rouse, J.W.; Haas, R.H.; Schell, J.A.; Deering, D.W. Monitoring vegetation systems in the great plains with ERTS. In *Earth Resources Technology Satellite (ERTS) Symposium*; NASA: Greenbelt, MD, USA, 1974.
19. Gitelson, A.A.; Kaufman, Y.J.; Merzlyak, M.N. Use of a green channel in remote sensing of global vegetation from EOSMODIS. *Remote Sens. Environ.* **1996**, *58*, 289–298. [CrossRef]
20. Sripada, R.P.; Heiniger, R.W.; White, J.G.; Meijer, A.D. Aerial color infrared photography for determining early in-season nitrogen requirements in corn. *Agron. J.* **2006**, *98*, 968–977. [CrossRef]
21. Wang, F.M.; Huang, J.F.; Tang, Y.L.; Wang, X.Z. New vegetation index and its application in estimating leaf area index of rice. *Rice Sci.* **2007**, *14*, 195–203. [CrossRef]
22. Nestel, D.; Dickschen, F.; Altieri, M.A. Seasonal and spatial population loads of a tropical insect: The case of the coffee leaf-miner in Mexico. *Ecol. Entomol.* **1994**, *19*, 159–167. [CrossRef]
23. Ahamed, T.; Tian, L.; Zhang, Y.; Ting, K.C. A review of remote sensing methods for biomass feedstock production. *Biomass Bioenergy* **2011**, *35*, 2455–2469. [CrossRef]
24. Souza, J.C.; Reis, P.R. *Bicho Mineiro: Biologia, Danos e Manejo Integrado*; Epamig 37; Júlio César de Souza: Belo Horizonte, Brasil, 1992.
25. Fragoso, D.B.; Jusselino-Filho, P.; Guedes, R.N.; Proque, R. Seletividade de inseticidas a vespas predadoras de *Leucoptera coffeella* (Guér.-Mènev.) (Lepidoptera: Lyonetiidae). *Neotrop. Entomol.* **2001**, *30*, 139–143. [CrossRef]
26. Marin, D.B.; Ferraz, G.A.E.S.; Guimaraes, P.H.S.; Schwerz, F.; Santana, L.S.; Barbosa, B.D.S.; Barata, R.A.P.; Faria, R.D.O.; Dias, J.E.L.; Conti, L.; et al. Remotely Piloted Aircraft and Random Forest in the Evaluation of the Spatial Variability of Foliar Nitrogen in Coffee Crop. *Remote Sens.* **2021**, *13*, 1471. [CrossRef]
27. Kagan, D.; Alpert, G.F.; Fire, M. Automatic large scale detection of red palm weevil infestation using street view images. *ISPRS J. Photogramm. Remote Sens.* **2021**, *182*, 122–133. [CrossRef]